Solar Energy Materials & Solar Cells 224 (2021) 110996

Contents lists available at ScienceDirect

Solar Energy Materials and Solar Cells

journal homepage: http://www.elsevier.com/locate/solmat

Lifetime prediction model of reflector materials for concentrating solar thermal energies in corrosive environments

Francisco Buendía-Martínez [a], Florian Sutter [b], Johannes Wette [b], Loreto Valenzuela [a], Aránzazu Fernández-García [a,*]

[a] CIEMAT-Plataforma Solar de Almería, Ctra. Senés, Km 4, P.O. Box 22, 04200, Tabernas, Almería, Spain
[b] DLR, German Aerospace Center, Institute of Solar Research, Paseo de Almería 73, 2, 04001, Almería, Spain

ARTICLE INFO

Keywords:
Renewable energy
Solar mirror
Corrosion
Lifetime prediction model
Accelerated aging
Durability

ABSTRACT

Concentrated solar thermal technologies play an essential role in the energetic transition which is currently facing our society. The energy generation in this technology vastly depends on the optical behaviour of the reflector materials of the solar field. Corrosion of solar reflectors might be an issue in locations with high corrosive environments because an excessive corrosion of the solar mirror could be catastrophic for the profitability of the concentrated solar thermal plant. This research is focusing on modelling the durability of four different solar reflector materials exposed outdoors by accelerated aging tests. For this purpose, ten locations suitable for concentrating solar thermal applications were classified depending on their corrosive aggressiveness. Commercial, free-lead and low-cost reflectors samples were exposed in all the sites to determine the influence of the corrosion in its durability. Corrosion defects appeared in the solar reflectors during outdoor exposure were properly reproduced by CASS test. Novel lifetime prediction models were developed for all the solar reflectors depending on the corrosive aggressiveness of the place. Number and thickness of the paint coatings employed in the solar mirrors were identified as one of the most important parameters to improve the energy generation of a CSP plant in corrosive environments. A reduction of the capital invested in the solar mirror purchase is expected for sites with low corrosivity.

1. Introduction

The increment of the greenhouse gases and the scarcity of fossil fuels have supposed a revolution in the energy field [1,2]. To tackle the required transition, renewable energies have been selected as the best alternative to lead the transformation to a new energy market, less harmful for the environment [3,4]. Among all renewable energies, solar technologies are considered as the most promising options because their environmental impact is almost negligible [5]. Especially, solar thermal energy (STE) is fundamental in the new energetic market because this technology is able to dispatch energy at any time of the day, thanks to thermal storage systems [6–8]. Nowadays, the worldwide installed capacity of concentrating solar power (CSP) plants is 5.5 GW, from which 42% is installed in Spain [9]. Besides, CSP systems generate 3% of the electricity generation mix of Spain. In accordance with the International Energy Agency (IEA) forecast [10], CSP energy is predicted to represent 11% of the total worldwide electricity generated in 2050. In addition, the International Renewable Energy Agency (IRENA) reported that CSP average levelized cost of electricity (LCOE) in 2018 was 0.186 €/kWh, 26% less than in 2017, and it is expected that in 2022 the LCOE will drop below 0.10 €/kWh [11].

The durability of the materials used in CSP systems is one of the main aspects to take into consideration during the design of a solar power plant. Solar plants are usually designed for a lifetime of at least 25 years. In this context, the solar field reflectors must preserve their initial optical behaviour for the whole duration of the solar plant with minimum degradation. This component is fundamental for the CSP plant performance because it is responsible to concentrate the solar radiation onto the receiver target. If this material fails, all the energy conversion process of the power plant will be affected [12]. Also, the purchase of the solar reflectors represents around 6.4% of the initial investment of a CSP plant [13], and their replacement is not contemplated during the lifetime of the facility. Silvered-glass mirrors are usually employed for CSP technologies due to their suitable optical behaviour and durability. Innovative low-cost and free-lead mirrors are being manufactured in order to reduce the capital invested for its purchase and to be more environmentally friendly. However, its durability is still unknown and

* Corresponding author.
E-mail address: arantxa.fernandez@psa.es (A. Fernández-García).

https://doi.org/10.1016/j.solmat.2021.110996
Received 21 July 2020; Received in revised form 26 January 2021; Accepted 3 February 2021
Available online 15 February 2021
0927-0248/© 2021 The Authors. Published by Elsevier B.V. This is an open access article under the CC BY-NC-ND license (http://creativecommons.org/licenses/by-nc-nd/4.0/).

Nomenclature

Acronyms

CASS	Copper-accelerated acetic acid salt spray
CSP	Concentrating solar power
DNI	Direct normal irradiance
EDX	Energy dispersive and X-ray
IEA	International Energy Agency
IRENA	International Renewable Energy Agency
ISO	International Organization for Standardization
LCOE	Levelized cost of electricity
LCOM	Levelized cost of the mirrors
MED	Multi-Effect distillation
NSS	Neutral salt spray
SEM	Scanning electron microscopy
STE	Solar thermal energy

Symbols

a	Solar-weighted hemispherical degradation rate ((−)/year)
af	Acceleration factor (−)
$\frac{A_{NC}}{A_{Total}}$	Ratio of non-corroded (or useful) area to the total area (−)
$\frac{A_C}{A_{Total}}$	Ratio of corroded area to the total area (−)
D	Reflective area of the solar field (m2)
$I_{t,\ reflector}$	Investment expenditures of the solar field considering a certain material reflector in the year t (€)
$M_{t,reflector}$	Operation and maintenance expenditures of the solar field considering a certain material reflector in the year t (€)
n	Expected lifetime of the CSP plant (years)
R^2	Adjusted R squared (−)
$t_{chamber}$	Time in of the accelerated aging test (hours)
$t_{outdoor}$	Time in outdoor (years)
ρ_0	Initial reflectance (−)
ρ	Total reflectance (−)
$\rho_{t,reflector}$	Total reflectance of a certain reflector in the year t (−)
ρ_{NC}	Reflectance in the non-corroded area (−)
ρ_C	Reflectance in the area corroded by spots (−)
$\rho_{s,\phi}(SW,\theta_i,\phi)$	Solar-weighted specular reflectance (−)
$\rho_{\lambda,\phi}(\lambda,\theta_i,\phi)$	Monochromatic specular reflectance (−)
$\rho_{s,h}(SW,\theta_i h)$	Solar-weighted hemispherical reflectance (−)

the performance of the CSP plant should not be affected for its implementation.

Corrosion has been identified as one of the main degradation mechanisms which might affect the durability and the optical behaviour of solar mirrors [14]. Some CSP plants are located in a corrosive atmosphere originated by saline environments. For example, for water desalination applications, CSP + MED (multi-effect distillation) plants need to be located near to the coast because it is not profitable to transport the exhaust steam over long distances due to the fact that excessive pipe diameters are required for this purpose [15,16]. Additionally, some places such as the Atacama Desert reported corrosion environments at night provoked by a sea fog, called “Camanchaca”, which penetrates into the desert during some periods of the year [17]. Also, there are some CSP plants already built near to the sea where corrosion issues could appear in the future. For instance, Noor Energy 1 PSC (Dubai) is situated around 50 km from the sea in air-line distance. In all these situations, reflectors will be subjected to harsh corrosive environment and it is vital to study their durability in order to predict the proper performance of the CSP system and anticipate corrective measures during the installation, operation and maintenance of the system.

Previous studies about corrosion degradation in industrial environments were carried out for primary reflectors [18–21]. Those publications reveal that the corrosion provoked by harmful agents originated in industrial atmospheres (SO_2, NO_2, H_2S …) might significantly affect the optical properties and also the durability of materials. Besides, studies about metal corrosion (especially copper and silver) in corrosive ambient are quite useful for understanding the possible corrosive degradation mechanisms and the sub-products formed in the metallic layers of the solar mirrors [22–25]. Then, it is also fundamental to estimate the lifetime of solar mirrors in places prompt to suffer corrosion due to high salinity.

One of the most common manners to predict the durability of a component is by exposing the material for a long time in the place where the CSP system will be installed. However, in many occasions the companies do not have enough time to expose material samples for a long time and decisions such as, which is the most suitable material, should be taken before starting the construction of the CSP plant. This problem is solved by using accelerated aging tests which reproduce the same degradation effects observed outdoors, but in a short period of time. Many accelerated aging tests have been used in recent works in order to simulate humidity and corrosive conditions for primary mirrors [26,27] and most of them are compiled in the Spanish standard for solar reflectors UNE 206016:2018 [28]. Neutral salt spray (NSS) and copper-accelerated acetic acid salt spray (CASS) tests stand out above the rest to reproduce corrosive environments [29]. Actually, CASS and NSS tests are commonly used in the automotive industry to assess the durability of their paints in corrosive environments. In both aging tests, chemical agents are added to the spray solution to create a corrosive ambient inside the chamber.

Once a proper accelerated aging test which reproduces the same degradation mechanisms observed outdoors is found, correlation models to outdoor exposure must be determined to calculate how much the aging test is accelerating the weathering observed outdoors. Exponential expressions such as Arrhenius, Butler–Volmer or Avrami equations have been utilized to model the durability of some new components [30–32], even primary mirrors [33,34]. In these last two works, the exponential equations showed acceptable agreement with the experimental data, including proper description of boundaries (such as the conditions of initial reflectance and converging to 0 for infinite exposure time). However, in both cases the study addressed alternative reflector materials (aluminium and polymer film mirrors), but there is a lack of knowledge with respect to lifetime predictions of the most commonly used reflector materials (silvered-glass mirrors).

This work is focused on modelling the lifetime of silvered-glass primary reflectors submitted to corrosive ambient. The corrosivity class according to ISO 9223:2012 [35] of several representative sites to build a CSP plants was determined. Samples of four different solar reflector materials were exposed in each location. Finally, the durability along the time was predicted for the different reflectors studied in all the places where the effect of the corrosion is significant by using accelerated aging tests.

2. Materials and methods

This section addresses a description of the different reflector materials used in this work, the procedures to expose the samples in outdoor conditions and to classify the sites depending on their corrosive aggressiveness, the accelerated aging test performed to properly reproduce corrosion, and the analysis carried out to assess the degradation of the reflectors. Also, the empirical expressions to achieve a model between outdoor exposure and accelerated aging test are explained.

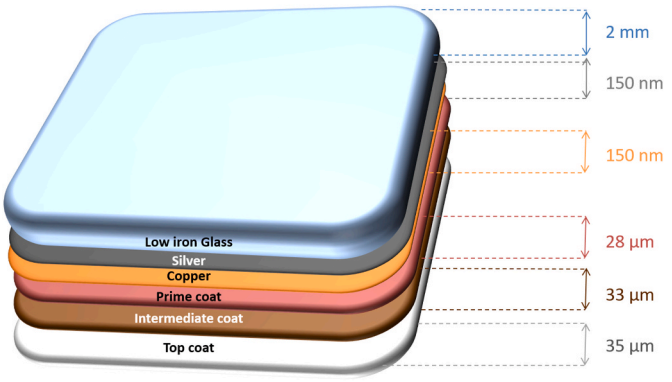

Fig. 1. Scheme of the silvered-glass reflector with 3 back paint layers (RLA1 material).

Finally, the procedure is described to perform an economic analysis to compare the cost of the materials tested, taking the price of the commercial one as a reference.

2.1. Reflector materials

Silvered–glass mirrors were selected for this work rather than aluminium ones. The reason is that the vast majority of CSP plants use silvered-glass mirrors because their initial optical performance is significantly higher [36] and they have shown excellent durability. Four silvered-glass reflector types manufactured by a highly experienced company were included in this study. These reflectors are composed by a silver reflective layer protected on the front by a thick glass layer and on the back by a copper layer and several paint coatings. Samples of 10 × 10 cm^2 (2 mm thickness) were cut from real-size facets of each material to be exposed in outdoors and tested in the accelerated aging experiments. All the samples had one original edge, coming from the real-size facet, and three cut edges.

The silvered-glass reflector materials studied are described as follow:

The commercial one (named RLA1), whose protective back system is composed by three paint layers with a thickness of 28, 33 and 35 μm (from the prime, intermediate and top coats, respectively) (Fig. 1). The cost of this material is taken as reference in the economic analysis (see Section 2.6).

- A reduced prototype of the commercial one (named RLA1R), whose paint layers are thinner in comparison with its commercial counterpart (the paint layers have a thickness of 22, 27 and 28 μm). Its cost is similar to RLA1.
- An innovative low-lead reflector (named RLA3) with two paint layers in which the lead content is negligible (the thickness of the paint layers are 31 and 35 μm). The price of this reflector is quite more expensive compared with RLA1.
- A low-cost reflector (named RLA4R) with only two paint layers (both with a thickness of 30 μm). This reflector is estimated to be 3% cheaper than RLA1.

Composition and thickness of the glass, silver and cooper layer was the same for all the materials.

2.2. Outdoor exposure test

Five samples of each reflector material were exposed in 10 representative sites with different climatic conditions. The places chosen to install the reflector samples were 3 in Europe (Tabernas and Almería in Spain, and Odeillo in France), 5 in North-Africa (Missour, Erfoud, Zagora, Ouarzazate and Temara in Morocco), and 2 in South-America (Atacama Desert and Chajnantor in Chile). In the Northern hemisphere's locations, the samples were located in a south facing rack with a tilt of 45° (marked in yellow in Fig. 2), which are typically selected in this kind of studies [37]. The samples exposed in South-America were facing north direction instead of south. During three years, one sample per material was yearly collected to be analysed in the laboratory. The characteristics of the different sites are summarized in Table 1:

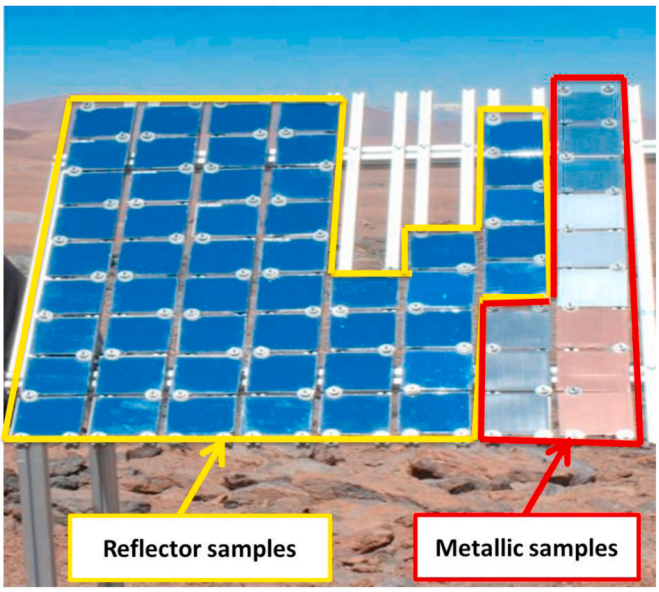

Fig. 2. Example of the reflector and metallic samples in the outdoor exposure test benches.

Table 1
Characteristics of the sites where reflectors samples were exposed.

Site	Coordinates	Climate	Distance to the coast in straight line (km)	Altitude (m)	Outdoor exposure time (months)
Almeria (Spain)	(36.8°N, 2.4°W)	Semiarid	0.5	0	34
Tabernas (Spain)	(37.1°N, 2.3°W)	Semiarid	30	404	33
Odeillo (France)	(42.5°N, 2°E)	Continental	100	1550	36
Missour (Morocco)	(32.8°N, 4.1°W)	Semiarid	290	1161	36
Erfoud (Morocco)	(31.5°N, 4.2°W)	Arid	380	822	36
Zagora (Morocco)	(30.3°N, 5.8°W)	Arid	360	727	36
Ouarzazate (Morocco)	(30.9°N, 6.9°W)	Arid	260	1126	24
Temara (Morocco)	(33.9°N, 6.9°W)	Semiarid	0	0	24
Atacama Desert (Chile)	(24.1°S, 70°W)	Arid	60	965	36
Chajnantor (Chile)	(23°S, 67.8°W)	Arid	270	5200	36

In order to identify the corrosive aggressiveness of the sites, the corrosivity class of each location was determined according to the ISO 9223:2012 standard [35]. For this purpose, 3 replicates of metal coupons (10 × 10 cm^2) of steel, copper, zinc and aluminium were exposed for 1 year at the same exposure sites (marked in red in Fig. 2), together with the reflector samples. Previously, in the laboratory, these coupons were weighted with a high precision balance to determine the initial

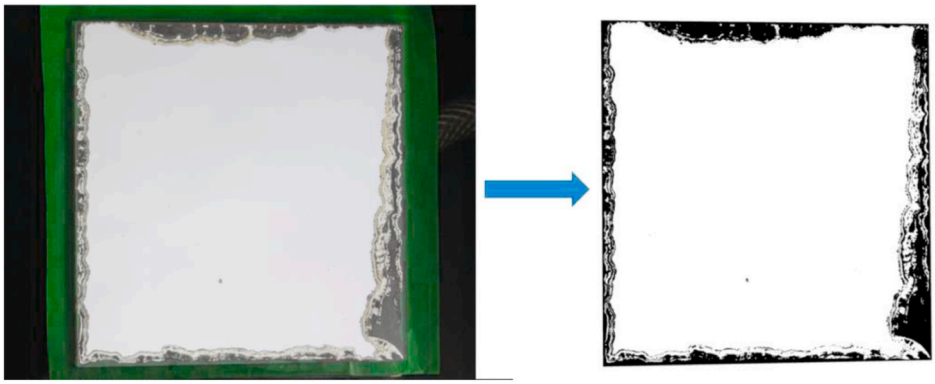

Fig. 3. Example of transformation of a picture of a reflector sample to a binary image with an image treatment software.

weight of the samples. After 1 year of outdoor exposure, the metals were collected, cleaned and weighted again in the laboratory. With this procedure, the sites were classified depending on the average weight loss per year of the metal coupons in 6 different categories (C1, C2, C3, C4, C5 and CX), where C1 means a site with slight corrosion and CX means a place with an extreme corrosive environment.

2.3. Accelerated aging test

The same corrosion defects happening outdoors must be reproduced through accelerated aging tests to obtain a suitable correlation [38]. In this way, a previous test campaign involving up to 12 different aging tests (NSS, damp-heat, CASS ….) was carried out with the same solar reflector in order to determine the most reliable test for simulating corrosion [39]. According to the results obtained, the CASS was chosen to reproduce corrosion because the same defects observed on exposed samples (such as corrosion spots or edge corrosion) were simulated in a short period of time (see subsection 3.2). An additional erosion test [37] applied on the back side of the reflectors might be recommended before the CASS test to provoke a pre-damage in the back paint coatings to reproduce the combined effect of erosion and corrosion, simulating the extreme ambient conditions of desert sites which are also close to the coast. This combined test was not considered in this work because it is exclusively focused on corrosive environments, but it is highly recommended for further studies.

CASS test was applied in accordance with the UNE 206016:2018 and ISO 9227:2017 standards [28,29]. The samples were sprayed with an aqueous solution mixed with [NaCl] = 50 g/l and [$CuCl_2$] = 0.26 g/l. The pH of the solution remains between 3.1 and 3.3. The test was carried out with a temperature, T, of $T = 50\ ^{\circ}C$ and relative humidity, RH, of $RH = 100\%$. The samples were tested for 2040 h and each 5 days (120 h) they were taken from the CASS chamber for analysis. Two days were needed to characterize all the samples and during this period they were kept under ambient conditions. After the two days of analysis, the reflectors returned to the chamber for another 5 days of aging.

2.4. Analysis techniques

Several optical analyses were periodically carried out both in the outdoor test (yearly) and in the accelerated aging test (weekly) to assess the parameters used in the correlations. The main parameter to determine the optical quality of a solar reflector is the reflectance [40]. Consequently, the prediction model proposed in this work is based on this parameter. The reflectance of a mirror , ρ, might be affected by the appearance and growth of corrosion spots because the reflection in corroded zones is significantly lower than in non-corroded zones [41]. For this reason, the ρ depends on the value measured both in the useful area (non-corroded)ρ_{NC}, and in the area corroded by spots, ρ_C. The reflectance measured in both zones is weighted by the corresponding areas, as it is represented in Eq. (1).

$$\rho = \rho_{NC} \cdot \frac{A_{NC}}{A_{Total}} + \rho_C \cdot \frac{A_C}{A_{Total}} \tag{1}$$

Where:

ρ denotes the total reflectance
ρ_{NC} denotes the reflectance in the non-corroded area
$\frac{A_{NC}}{A_{Total}}$ denotes the ratio of non-corroded (or useful) area to the total area
ρ_C denotes the reflectance in the area corroded by spots
$\frac{A_C}{A_{Total}}$ denotes the ratio of area corroded by spots to the total area
As ρ_C is negligible (the reflectance of the corrosion spots can be assumed to be close to zero), Eq. (1) can be simplified to Eq. (2):

$$\rho = \rho_{NC} \cdot \frac{A_{NC}}{A_{Total}} \tag{2}$$

And as $\frac{A_{NC}}{A_{Total}}$ can be written as $(1 - \frac{A_C}{A_{Total}})$, then:

$$\rho = \rho_{NC} \cdot \left(1 - \frac{A_C}{A_{Total}}\right) \tag{3}$$

To compute ρ over time, two main parameters need to be obtained. Firstly, several reflectance measurements were periodically performed in the non-corroded area in order to calculate the ρ_{NC}. The solar-weighted specular reflectance, $\rho_{s,\phi}(SW,\theta_i,\phi)$, is the most representative parameter to assess the optical behaviour of a solar mirror. According to Ref. [42], the solar specular reflectance can be indirectly calculated by measuring the monochromatic specular reflectance, $\rho_{\lambda,\phi}(\lambda,\theta_i,\phi)$ and the solar-weighted hemispherical reflectance, $\rho_{s,h}(SW,\theta_i,h)$. While $\rho_{\lambda,\phi}(\lambda,\theta_i,\phi)$ was measured at $\lambda = 660$ nm, $\theta_i = 15^{\circ}$ and $\phi = 12.5$ mrad with a portable specular reflectometer model 15 R–USB manufactured by D&S, $\rho_{s,h}(SW,\theta_i,h)$ was calculated by measuring the spectral hemispherical reflectance, $\rho_{\lambda,h}([\lambda_a,\lambda_b],\theta_i,h)$, at $\lambda = [320, 2500]$ nm and $\theta_i = 8^{\circ}$ with a spectrophotometer model Lambda 1050 manufactured by Perkin Elmer [43,44], and applying the weighting formula included in the ISO 9050:2003 standard [45] with the solar spectrum from the ASTM G173-03 standard [46]. Monochromatic specular reflectance was measured in 5 different points of the solar mirror, randomly distributed on the reflector area exempted of corrosion. These measurements were performed both before and after the tests by the same operator and maintaining the same ambient conditions to minimize the measurement uncertainties. The same methodology was utilized to quantify the solar-weighted hemispherical reflectance, but measuring 3 points instead of 5.

Secondly, a picture of the whole sample surface was taken to determine $\frac{A_C}{A_{Total}}$. In this picture, it was possible to distinguish between the corroded area originated by the appearance and growth of corrosion

spots and the corroded area which came from the original and cut edges. In this study, only the corrosion caused by the corrosion spots was taken into consideration because the degradation originated in the cut edges is not realistic from real plant conditions, in which all the edges are protected. The corrosion of the cut edges also affects to the original edges. Therefore, corrosion provided from the edges is not taken into account. The real image was converted into a binary picture with an image processing software to calculate the corroded area. Corrosion was detected in black, while non-corroded area was observed in white (Fig. 3). Moreover, microscopic pictures were taken with an optical microscope model Axio XSM 700 manufactured by Zeiss in order to follow the evolution of the microscopic defects appearing along the surface.

In addition, the characterization of the degradation mechanism was accomplished. Scanning Electron Microscopy-Energy Dispersive and X-ray spectroscopy (SEM-EDX) were performed with a SEM manufactured by Hitachi, coupled with a QUANTAX -EDX system manufactured by Bruker. The reflectors were scanned with electron beams in order to obtain high-resolution black and white images which allow the study of the surface morphology. Besides, this technique is able to provide the elemental analysis of the surface studied. A cross section of one reflector sample was carried out just in the area of a corrosion spot to be analysed in the SEM-EDX. The elemental composition of the corroded area was determined. The results obtained in the corroded area were compared with the non-corroded area in order to identify the chemical agents that provoked the corrosion of the silver reflective layer.

2.5. Correlation approach

A degradation model was established to estimate ρ throughout the time in real operating conditions (Eq. (3)) by using the results obtained in the CASS test and outdoor exposure. As it is noticed in Eq. (3), ρ depends on two fundamental parameters, ρ_{NC} and $\frac{A_C}{A_{Total}}$.

ρ_{NC} might decrease along the time in outdoor exposure because of other environmental effects which deteriorate the glass surface, such as erosion, UV degradation, soiling deposition. The effects of the degradation mechanisms different to the corrosion were considered by measuring every year the reflectance evolution in the useful area of the samples exposed in outdoors. Supposing that ρ_{NC} has a linear degradation rate over the time (it has been shown in other works that another main degradation mode is erosion of the glass surface and this effect can be regarded as linear [47,48]), then, ρ_{NC} will be:

$$\rho_{NC} = \rho_0 - a \cdot t_{outdoor} \tag{4}$$

Where:

ρ_0 denotes the initial reflectance
a denotes the solar specular reflectance degradation rate.
$t_{outdoor}$ denotes the time in outdoor

With regards to the second term of Eq. (3), $\frac{A_C}{A_{Total}}$, the corrosion data obtained in the CASS test was plotted as function of the time to achieve the most suitable fit which simulates the tendency of this parameter. According to the experimental results (see section 3.4), it was assumed that the area corroded by spots can be described by the Avrami equation (Eq. (5a)), which gives the fraction of corroded area after a certain test time in the ageing chamber:

$$\frac{A_C}{A_{Total}} = 1 - e^{-b(t_{chamber})^c} \tag{5a}$$

Where:

$\frac{A_C}{A_{Total}}$ denotes the ratio of area corroded by spots to the total area.
$t_{chamber}$ denotes the time of the accelerated aging test
b and c are two fitting constants obtained through the accelerated aging test data.

Exponential equations can be transformed into a linear expression by using Naiperian logarithms. The interception with the y axis determines the ln b and the slope of the line represents the parameter c. Then, Eq. (5a) can be rewritten as:

$$\ln\left(\ln\left(\frac{1}{1 - A_C/A_{Total}}\right)\right) = \ln b + c \cdot \ln t_{chamber} \tag{5b}$$

It is assumed that the fitting parameters b and c obtained from the CASS test are also valid to model the corrosion evolution in outdoor conditions. But the corrosion process in outdoor evolves in a much slower time-scale. This effect is taken into account by including the acceleration factor, a_f, in Eq. (5a).

The a_f is defined as the ratio between the time necessary to obtain a stated proportion that an aging test accelerates a degradation mechanism in comparison with outdoors. In this case, a_f is obtained as the ratio of the time in outdoor exposure to the time in the CASS test, for the same area corroded by spots:

$$a_f = \frac{t_{outdoor}}{t_{chamber}} \tag{6}$$

Then, considering Eq. (6) in Eq. (5a), it can be rewritten as Eq. (7).

$$\frac{A_C}{A_{Total}} = 1 - e^{-b\left(\frac{t_{outdoor}}{a_f}\right)^c} \tag{7}$$

With Eq. (7), the evolution of the area corroded by spots can be calculated throughout the time for any primary mirror by obtaining the parameters b and c in the CASS test and the acceleration factor between any location and the CASS test. If $\frac{A_C}{A_{Total}}$ is replaced in Eq. (3) with the term obtained in Eq. (7), the following expression is found:

$$\rho = \rho_{NC} \cdot e^{-b\left(\frac{t_{outdoor}}{a_f}\right)^c} \tag{8}$$

Finally, combining Eq. (4) and Eq. (8) leads to a model that simulates the evolution of the reflectance of a solar reflector ρ, throughout the time for any location:

$$\rho = \left(\rho_0 - a \cdot t_{outdoor}\right) \cdot \left(e^{-b\left(\frac{t_{outdoor}}{a_f}\right)^c}\right) \tag{9}$$

2.6. Economic analyses

In order to evaluate the influence of the reflector material performance in the feasibility of the CSP plant, an assessing parameter is proposed, named levelized cost of the mirrors, LCOM. By similarity with the levelized cost of electricity (LCOE) [49], the LCOM is the ratio between the costs of the solar field mirrors divided by the energy delivered by the mirrors over the lifetime of a CSP plant, as it is indicated in Eq. (10).

$$\text{LCOM}\left(\frac{€}{\text{kW·h}}\right) = \frac{\sum_{t=1}^{n}\left(I_{t,reflector} + M_{t,reflector}\right)}{\sum_{t=1}^{n}\left(\rho_{t,\ reflector} \cdot DNI_t \cdot D\right)} \tag{10}$$

Where:

$I_{t,\ reflector}$ denotes the investment expenditures of the solar field considering a certain material reflector in the year t, in €
$M_{t,\ reflector}$ denotes the operation and maintenance expenditures of the solar field considering a certain material reflector in the year t, in €
$\rho_{t,\ reflector}$ denotes the ρ of a certain reflector in the year t.

Table 2
Average mass loss per square meter for the four metals coupons after 1 year of outdoor exposure and average corrosivity class of the sites.

Site	Average mass loss (g/m^2)				Average corrosivity class
	Zinc	Cooper	Aluminum	Steel	
Almeria	8.78	43.4	1.19	346	**C4**
Tabernas	3.79	15.3	0.45	132	**C3**
Odeillo	3.30	5.61	0.09	8.59	**C2**
Missour	5.05	7.62	0.14	43.4	**C2**
Erfoud	4.01	19.8	0.30	65.7	**C2**
Zagora	2.44	5.15	0.03	28.3	**C2**
Ouarzazate	3.75	7.15	0.47	19.4	**C2**
Temara	398	190	4.83	7769	**CX**
Atacama Desert	5.41	20.5	0.64	210	**C3**
Chajnantor	3.50	6.38	0.27	103	**C2**

DNI_t denotes the yearly sum of direct normal irradiance in the year t, in kW·h/m.^{2}
D denotes the reflective area of the solar field, in m.^{2}
n denotes the expected lifetime of the CSP plant.

The profitability of using low-cost materials instead of the commercial one is calculated by the relative LCOM. This parameter notices the percentage saved in the LCOM when some novelty reflector is compared with the commercial one (RLA1), and can be described by the next expression:

$$\text{Relative LCOM } (\%) = \frac{\frac{\sum_{t=1}^{n} I_{t,\ RLA1} + M_{t,RLA1}}{\sum_{t=1}^{n} \rho_{t,RLA1} \cdot DNI_t \cdot D} - \frac{\sum_{t=1}^{n} I_{t,reflector} + M_{t,reflector}}{\sum_{t=1}^{n} \rho_{t,\ reflector} \cdot DNI_t \cdot D}}{\frac{\sum_{t=1}^{n} I_{t,\ RLA1} + M_{t,RLA1}}{\sum_{t=1}^{n} \rho_{t,RLA1} \cdot DNI_t \cdot D}} \ x\ 100 \qquad (11)$$

A relative LCOM equal to 0% means that the reflector material type does not affect the financial aspects of the plant. If the relative LCOM of a certain reflector material is higher than 0% it means that a saving in the cost of the energy reflected is expected with respect to the commercial material, and if it is lower than 0%, just the opposite.

3. Results and discussion

This section includes the results of the corrosivity class of every site where reflectors samples were exposed, the characterization of the degradation mechanism happened during the corrosion and the evolution of the reflectance and corrosion both in outdoor exposure and in CASS conditions. Finally, the lifetime prediction of the optical behaviour and an economic study of the primary mirrors in corrosive environments were modelled along the time.

3.1. Corrosivity class of the tested sites

The corrosivity coupons were collected after 1 year of outdoor exposure and weighted in the laboratory. Average mass loss per square meter and the corresponding corrosivity class of all the sites studied are compiled in Table 2.

As it is shown in Table 2, the sites which are near to the coast (see Table 1) present higher corrosivity classes than the rest. Temara is an extremely corrosive site because the test bench was installed just in front of the sea. Primary mirrors exposed in Temara were corroded after several months because the corrosion penetrated through the cut edges and the primary mirrors were totally destroyed in less than one year of outdoor exposure [50]. Consequently, the results of Temara are not considered in this work because the corrosion took place in the cut edges and this kind of corrosion is not representative for real solar fields of CSP plants (where edges are properly protected). Then, Almería is the place with major corrosion (C4) followed by Tabernas and Atacama Desert (C3). Regarding C2 and C1 sites, it was determined that the corrosion is not a main degradation mechanism (at least for the testing time considered in this work) and the influence of this effect might be considered negligible. For this reason, only sites with a corrosivity class equal to or higher than C3 are studied in this work, that is, Almería, Tabernas and Atacama Desert.

3.2. Characterization of the degradation mechanism: corrosion

Fig. 4 represents two pictures of corroded samples of RLA4R reflectors, one after three years of outdoor exposure in Almería and another after 360 h in the CASS test. Both samples showed similar degradation mechanisms, such as corrosion spots and corroded edges. These defects appeared in the reflector as a consequence of the corrosion of the reflective silver layer. In the case of the cut edges, the silver was in direct contact with the corrosive agents, and for this reason it was perceived a great corrosion in these zones. However, the corrosion spots appeared because the corrosive agents penetrate through the paints layers (either by a physical damage suffered due to outdoor exposure or by the permeability of the paints) until reaching the silver layer. In this second situation, the quality, thickness and number of paint layers are fundamental to avoid the appearance of corrosion spots.

A previous study was performed to identify the chemical changes occurring in the silvered reflective layer of a reflector when the samples were submitted to saline environments in Newcastle (Australia) [51]. It

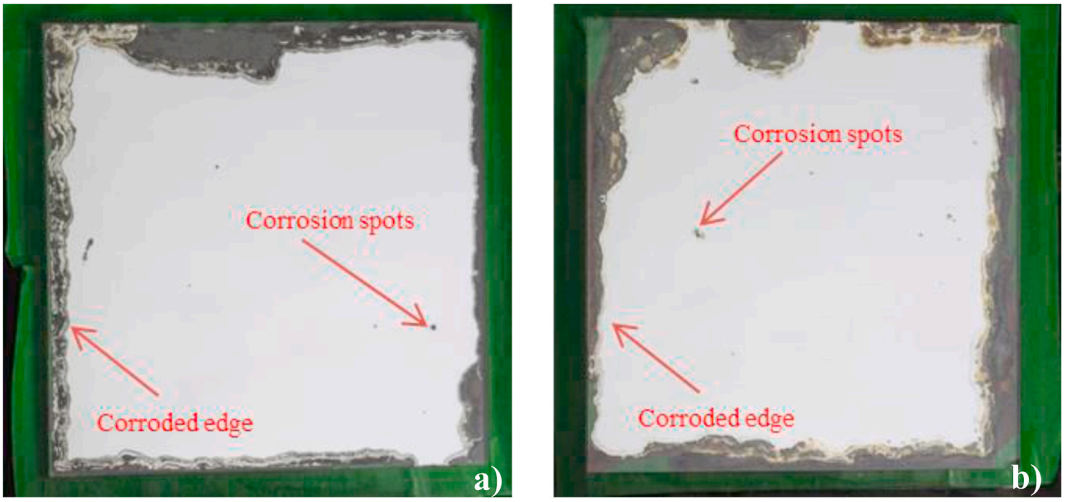

Fig. 4. Pictures of corroded samples of RLA4R reflectors: a) after approximately 3 years of outdoor exposure in Almería, b) after 360 h in CASS conditions.

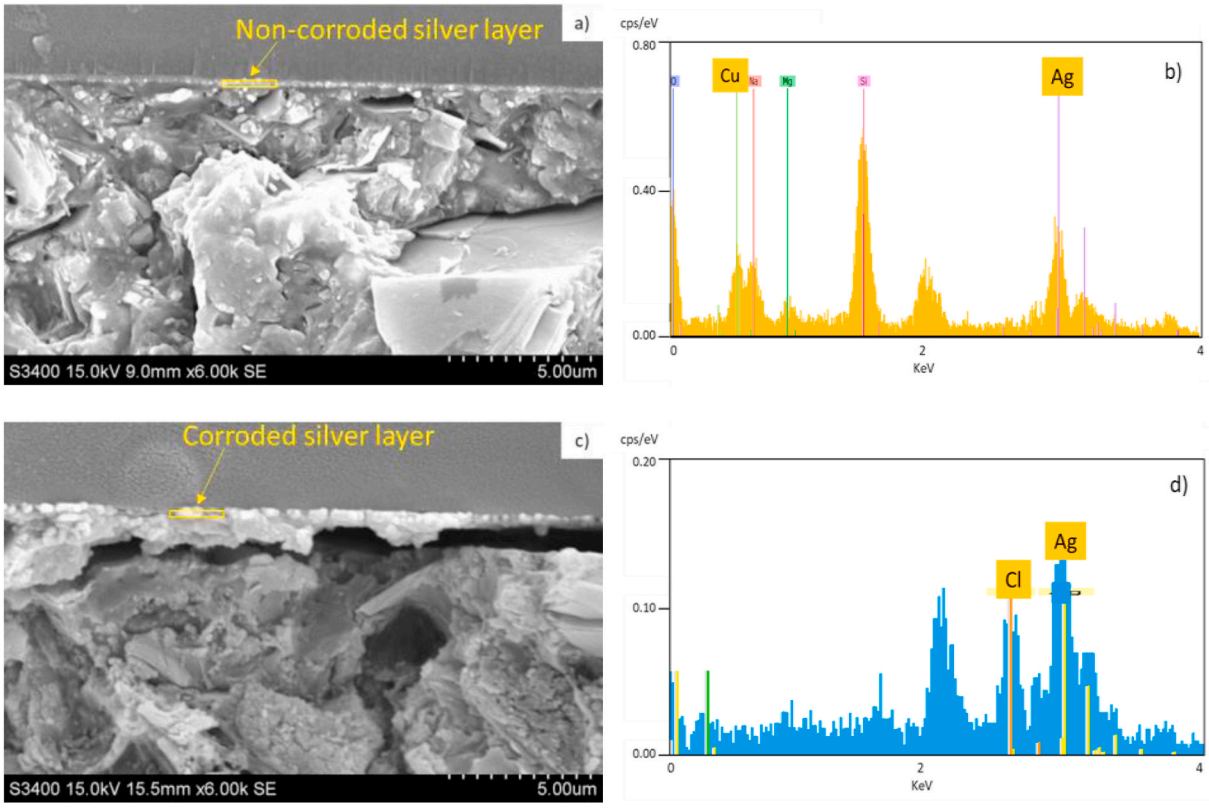

Fig. 5. SEM-EDX analysis of a cross-section in a non-corroded silver layer before any test, (a) and (b), and in a corroded silver layer after 360 h of the CASS test, (c) and (d).

was appreciated that the corroded parts of the reflectors possessed traces of chloride ions in the silver layer which could be associated to the corrosion of the material.

In this work, SEM-EDX analyses were carried out to reflector samples subjected to CASS conditions in order to verify that the same degradation mechanism happening outdoors is reproduced in the climate chamber. Fig. 5 illustrates the SEM-EDX analysis of a cross-section performed both in a non-corroded silver layer (at the initial status, before testing) and in a corrosion spot appearing after 360 h of CASS testing. The upper picture shows the SEM image of a non-corroded silver layer (a), where the dark area corresponds to the glass section, the bright area corresponds to the silver layer and the granulated area corresponds to the prime coat (see Fig. 1). The EDX spectrum measured in the region of the silver layer (yellow rectangle) is represented in the image b). The same procedure was performed for the corroded silver layer, where the SEM image is depicted in c) and the EDX results are represented in d).

The SEM-EDX analysis demonstrated the appearance of chloride ions in the silver layer after the CASS test. Cl^- ions reacted with the silver to form silver chlorides which significantly reduced the optical properties of the reflector. Also, it is very important to highlight that no copper was found on the sample after CASS testing. It is concluded that the copper acted as sacrificial anode, protecting the silver layer against the corrosion until its own dissolution. Once the copper was removed, the silver layer began to corrode.

Comparing the EDX results of the samples tested in CASS conditions with the results obtained in an outdoor site close to the coast [51], many similarities were perceived between both degradation mechanisms. Consequently, it is concluded that CASS test is a reliable aging test to simulate corrosion in solar reflectors.

3.3. Outdoor results

Table 3 compiles the average of the solar specular reflectance degradation rates per year, $\Delta\rho_{s,\phi}$ (parameter a of Eq. (9)), after 3 years of outdoor exposure for the reflector materials exposed in Almería, Tabernas and Atacama Desert.

Table 3
Degradation rate per year of the solar specular reflectance ($\Delta\rho_{s,\phi}$) (parameter a), depending on the material and site.

Material	Site (corrosivity class)		
	Almería (C4)	Tabernas (C3)	Atacama Desert (C3)
	$\Delta\rho_{s,\phi}$ ((−)/year)	$\Delta\rho_{s,\phi}$ ((−)/year)	$\Delta\rho_{s,\phi}$ ((−)/year)
RLA1	−0.0011	−0.0005	−0.0015
RLA1R	−0.0013	−0.0007	−0.0012
RLA3	−0.0009	−0.0004	−0.0013
RLA4R	−0.0013	−0.0007	−0.0012
Average	**−0.0012**	**−0.0006**	**−0.0013**

As it is observed in Table 3, Almería and Atacama Desert showed a values similar between them, and higher than Tabernas. In Almería, the ρ_{NC} was mainly affected by dust deposits, mixed with the salinity of the ambient, which were accumulated on the glass (see Fig. 6 a). However, in Atacama Desert, ρ_{NC} was altered by sand storms which eroded the glass (see Fig. 6 b). Furthermore, it is perceived that the materials had similar a values within the same sites. This is because all the materials possess the same type of glass in the front layer.

In addition, the ratio of corroded area provoked by the appearance and growth of corrosion spots was determined ($\frac{A_C}{A_{Total}}$ in Eq. (7)). Table 4 shows the ratio of the area corroded by spots after approximately 3 years of outdoor exposure.

As it was predictable, the nearer the location to the coast, the higher the amount of corrosion is. The samples in Almería were located very close to the sea (see Table 1), and for this reason, the area corroded by spots was reasonably higher compared with the rest of the sites.

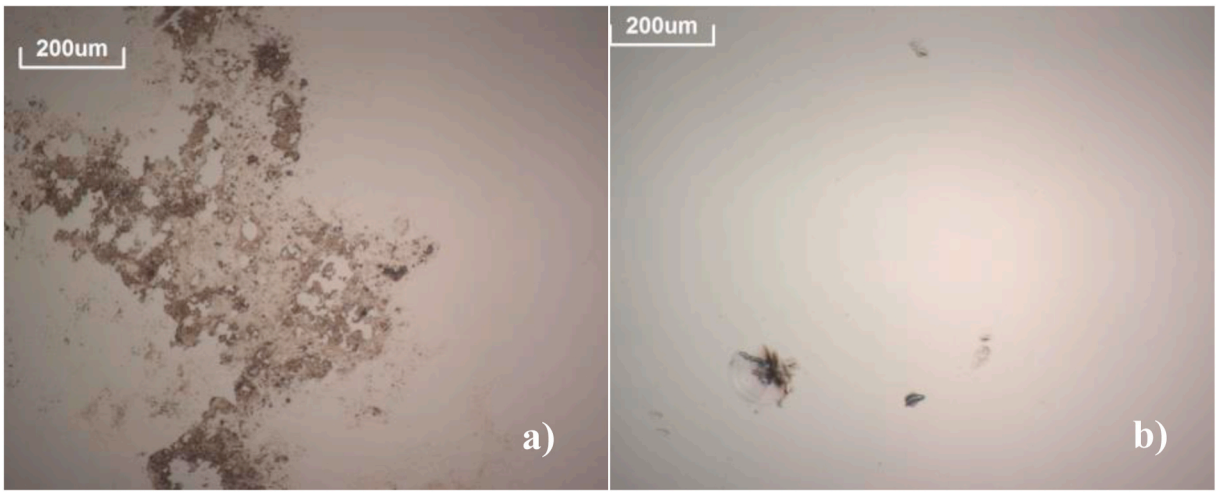

Fig. 6. Microscopic images of: a) dust deposits on the glass found in Almería, b) erosion of the glass detected in Atacama Desert.

Table 4

Ratio of area corroded by corrosion spots $\left(\frac{A_C}{A_{Total}}\right)$ after approximately 3 years of outdoor exposure, depending on the material and site.

Material	Site (corrosivity class)		
	Almería (C4)	Tabernas (C3)	Atacama Desert (C3)
	$A_C/A_{Total}(-)$	$A_C/A_{Total}(-)$	$A_C/A_{Total}(-)$
RLA1	0.000001	0.000000	0.000000
RLA1R	0.000007	0.000002	0.000002
RLA3	0.000037	0.000004	0.000001
RLA4R	0.000210	0.000021	0.000055

Comparing Tabernas and Atacama Desert, which possess the same corrosivity class and a similar distance to the coast in straight line (less than 100 km), it was appreciated similar corrosion levels in both sites, being in the Atacama Desert slightly higher.

Comparing the materials, RLA1 and RLA1R (both with 3 paint layers) exhibited the most suitable behaviour against the corrosion, being their corroded areas significantly smaller in all the locations than in the rest of reflectors. RLA4R (with 2 paint layers) looked as the weakest reflector against the corrosion because its corroded area was significantly higher. Finally, RLA3 (low-lead paints) displayed an intermediate behaviour. Focusing in the relevance of the thickness of the paint layers within the same type of reflector, it was observed that RLA1 was more protected against the corrosion than its counterpart with the thinner paint coatings (RLA1R). Then, it can be concluded that the number and thickness of paint layers play a fundamental role to avoid the penetration of the corrosion.

3.4. Accelerated aging results

As it is mentioned in subsection 2.3, all the reflectors were tested in the CASS chamber, and periodically measured each 120 h of testing time. The ratio of area corroded by spots is represented in Fig. 7 in function of the time in chamber. A zoom of the graph between 0 and 0.3% is depicted in the right-lower zone to properly observe the results of RLA1, RLA1R and RLA3 materials.

As it is illustrated in Fig. 7, at the beginning of the test, the corrosion in all the reflector samples is zero, while A_C/A_{Total} increased exponentially throughout the time in chamber. The slope of the curves is

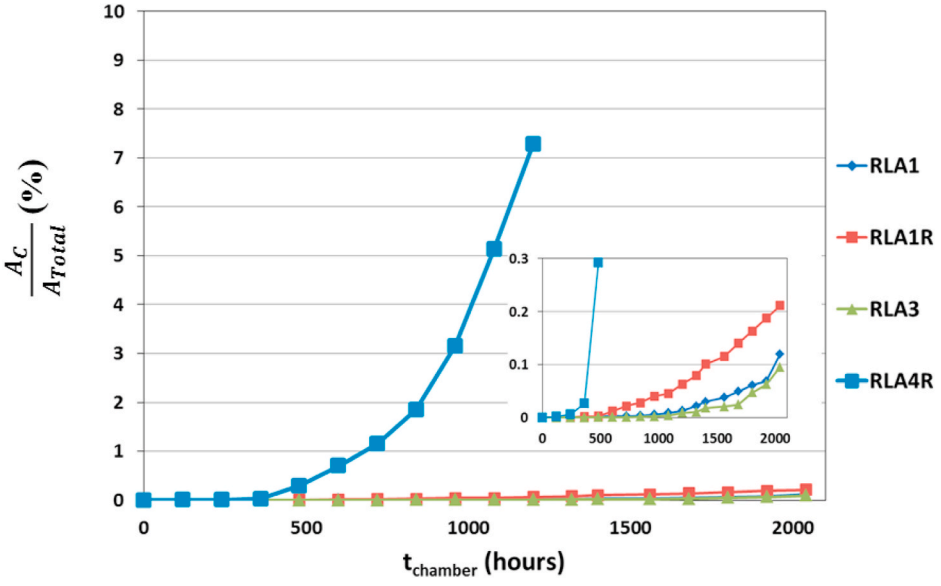

Fig. 7. Ratio of the area corroded by spots in the CASS test, depending on the material.

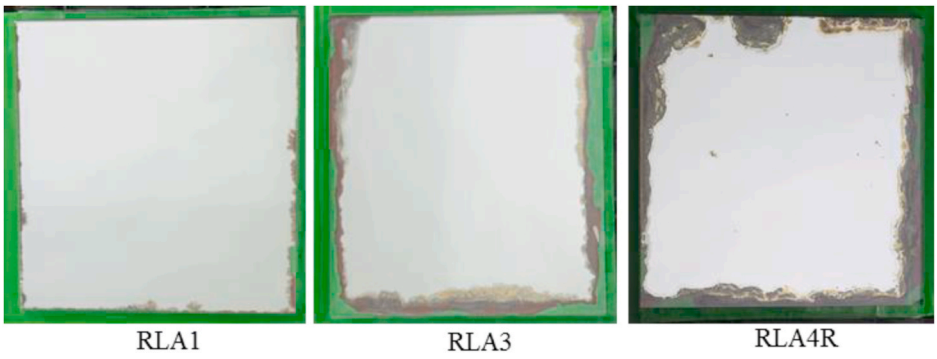

Fig. 8. Pictures of RLA1, RLA3 and RLA4R after 240 h of CASS test.

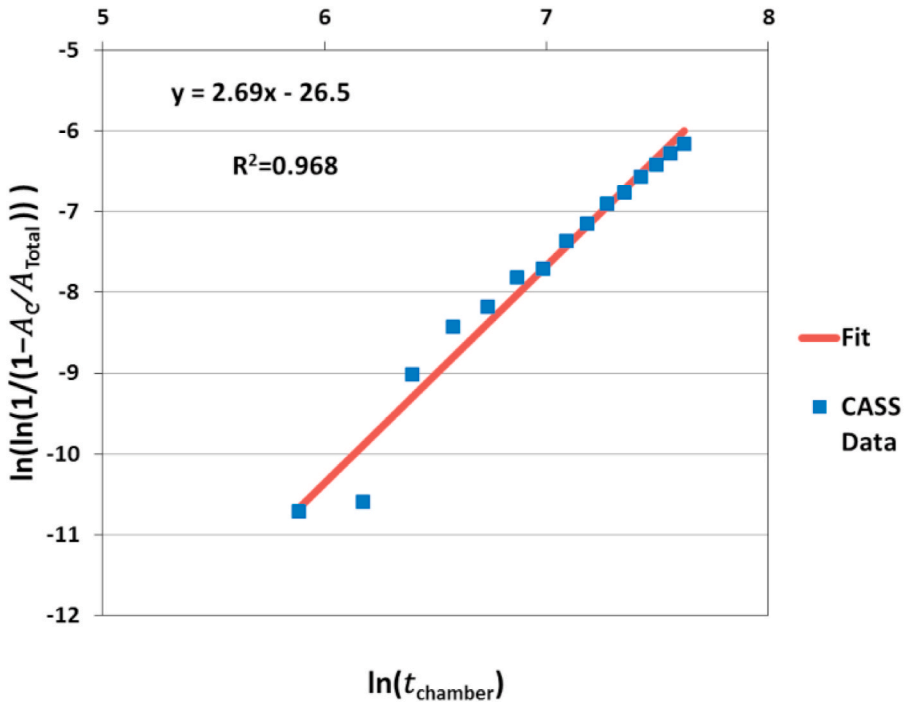

Fig. 9. Example of plotting and fitting of the CASS data for RLA1R (with -ln b = 26.5 (b = 3.1 × 10-12) and c = 2.69).

determined by the resistance of the reflector samples against the appearance of corrosion. As it is perceived, RLA1, RLA1R and RLA3 reflectors showed an exceptional resistance against the corrosion in comparison with the low-cost reflector (RLA4R). The reason of these corrosion differences is that RLA1 and RLA1R are formed by 3 paint layers, whereas RLA4R is composed by only 2. These results demonstrate that incorporating one more paint layer is fundamental to prevent the penetration of the corrosion to the silver layer. With respect to RLA3, it is only formed by two paint layers, but the composition is totally different because no lead was added to the paint coats. The behaviour of this material is extraordinary because its resistance is similar to the materials with 3 paint layers. Additionally, in Fig. 7 it is manifested that RLA1 showed a superior ability to prevent the penetration of the corrosion in comparison with its counterpart.

Fig. 8 depicts the type of corrosion appearing in RLA1, RLA3 and RLA4R after 240 h of CASS test. RLA1 suffered slight corrosion only in the non-protected edges, while the protected edge (the upper one) and the rest of the area are fully undamaged. With respect to RLA3 (low-lead 2 paint layers), there is not corrosion provoked by spots, but the edges are much more delaminated than in RLA1, especially the non-protected ones (all except the upper one). This delamination might be mitigated if all the edges were protected. About RLA4R, the appearance of a significant number of corrosion spots and the corrosion of the edges is the main issue of these reflectors.

Table 5
Fitting parameters (*b* and *c*) and adjusted *R* squared obtained from the CASS test results, depending on the material.

Material	Parameter		
	b (−)	*c* (−)	R^2 (−)
RLA1	2.6e-13	2.87	0.958
RLA1R	3.1e-12	2.69	0.968
RLA3	1.7e-15	3.48	0.942
RLA4R	3.4e-14	4.01	0.970

Data of the area corroded by spots obtained in CASS test (Fig. 7) were linearized by using Napierian logarithm (see Eq. (5b)). A linear fit was carried out to calculate the constant *b* and *c* of each material. As an example, Fig. 9 shows the good agreement observed between the linear fit and the experimental data for the RLA1R material during CASS testing. Table 5 compiles the parameters *b*, *c* and R^2 obtained for each material.

Table 6
Time in chamber ($t_{chamber}$) that simulates the same area corroded by spots $\left(\frac{A_C}{A_{Total}}\right)$ after approximately 3 years of outdoor exposure and the acceleration factor (a_f) between the CASS test and outdoor exposure, depending on the material and site.

Material	Site (corrosivity class)					
	Almería (C4)		Tabernas (C3)		Atacama Desert (C3)	
	$t_{chamber}$ (h)	a_f (−)	$t_{chamber}$ (h)	a_f (−)	$t_{chamber}$ (h)	a_f (−)
RLA1	234	106	118	204	131	200
RLA1R	230	108	130	185	144	182
RLA3	935	27	493	48	331	79
RLA4R	280	88	157	153	201	131

3.5. Lifetime prediction

The lifetime prediction results of the four materials studied in the three goal sites are presented in this section. The $\left(\frac{A_C}{A_{Total}}\right)$ in outdoor (see Table 4) are replaced in Eq. (5a) to calculate the $t_{chamber}$ invested in CASS test to reproduce the same corroded area appeared in outdoor exposure after approximately 3 years. Once $t_{chamber}$ and $t_{outdoor}$ are known for the same corroded area, the a_f (see Eq. (6)) is calculated. Results of $t_{chamber}$ and a_f for each material are compiled in Table 6.

As it is exposed in Table 6, a_f are significantly lower in Almería (C4) than in the other two sites (C3). This happens because the area corroded by spots in Almería after 3 years of outdoor exposure is higher (see Table 4) and more hours of CASS test are needed to reproduce the same amount of corrosion, that is to say, the corrosive atmosphere in this place is the most severe. Regarding Atacama Desert and Tabernas, both places share similar a_f because the corrosivity classes of the sites are equals.

If the parameters a (see Table 3), b and c (see Table 5), and a_f (see Table 6) are inserted in Eq. (9), the ρ can be calculated throughout the time. Lifetime prediction for 20 years is provided in Fig. 10 for all the materials and sites.

As it is observed, low-cost reflector (RLA4R) is not appropriate to be installed in a C4 sites such as Almería because it is expected that in less than 10 years, its optical performance will decrease more than the 5% of their initial performance (which is established as the maximum acceptance criterion in previous works [52]). For sites with high corrosive aggressiveness such as Almería, it is recommended to use reflectors with 3 paint layers (RLA1 and RLA1R) which mightily protect against the appearance of corrosion in the silver layer.

With respect to the C3 sites, the estimated reflectance losses for all the materials are insignificant for almost 10 years. After 20 years of operating conditions, reflectance drops values lower than 3% of their initial performance are expected for RLA1, RLA1R and RLA3. Regarding RLA4R material, the predicted reflectance approximately falls a 7% and 11% of its initial performance after 20 years in Tabernas and Atacama Desert, respectively. Besides, the employment of lead-free materials (like RLA3) in these places is feasible in the coming future from the point of view of their behaviour, if severe regulations about the amount of lead in the paints are imposed by the governments.

Finally, in accordance with the results of the predicted reflectance, RLA1 and RLA1R are two materials which are not substantially affected by the corrosion neither in a C4 nor in a C3 site. However, it is perceived that the reflectance decreases in Almería and Antofagasta more than in Tabernas (around 1% more after 20 years). The explanation of these optical differences is found in the influence of the dust deposits accumulated on the glass surface in Almería and the erosion of the glass originated by sand particles in Atacama Desert.

3.6. Economic analyses

The relative LCOM is calculated in this section for RLA1R and RLA4R materials, by using Eq. (11). RLA3 is not included in this analysis because the price of this reflector is considerably higher than the price of RLA1 and its durability is worse. As it is mentioned in subsection 2.1, RLA1R price is similar to RLA1 ($I_{RLA1R} = I_{RLA1}$), and RLA4R price is 3% less than RLA1 ($I_{t,RLA4R} = 0.97 \cdot I_{t,RLA1}$). As the parameters $M_{t,reflector}$, D and DNI_t are identical for all the materials and $\rho_{t,refletor}$ throughout the time was predicted in subsection 3.5, the relative LCOM over the time is depicted in Fig. 11 depending on the material and site.

As it is shown in Fig. 11, low-cost material (RLA4R) might be a suitable option in C3 sites (Tabernas and Atacama Desert) because a saving of approximately 2% in the LCOM is expected after 20 years of outdoor exposure. However, in Almería (C4), low-cost reflectors are only advisable to be used if the expected plant lifetime is less than 15 years. If a longer plant lifetime is targeted, the commercial material is the most suitable alternative. The differences among RLA1 and RLA1R are negligible and both reflectors could be used indistinctly. Consequently, a reduction of the thickness of the paint layers may be admissible.

4. Conclusions

One of the main degradation mechanisms observed in the primary reflectors installed in corrosive environments is the corrosion of the silver layer. Corrosion was accurately reproduced under accelerated aging conditions by the CASS test and was therefore selected as the most suitable aging test to simulate corrosive environments.

Lifetime prediction models between CASS test and outdoors were developed to estimate the reflectance evolution of four silvered-glass reflector materials in sites with corrosivity classes C3 and C4, where the corrosion can be affect to the energy generation of the CSP plant. Taking into account the optical behaviour and the cost of the solar reflectors, it is concluded that in C3 sites, it is expected a significant reduction of the capital invested for the purchase of the solar field because it is possible to use some low-cost reflectors for more than 20 years of outdoor exposure. However, considerable degradation is expected for low-cost reflector materials after 15 years of exposure in C4 environments, affecting to the optical behaviour, and therefore, to the performance of the CSP plant. For sites with high corrosive environments, it is recommended to use reflectors with 3 paint layers because they properly preserve its optical characteristics over the time.

Acceleration factors (a_f) between CASS test and C3 and C4 outdoor sites (after three years of outdoor exposure) are established in this work. Considering the results of the commercial material (RLA1) as the most representatives, the a_f calculated are 106 for Almeria (C4), 204 for Tabernas (C3) and 200 for Atacama Desert (C3). The acceleration factors and the lifetime models obtained in this paper involve a useful tool to predict the durability of new solar reflector materials submitted to corrosive environments, guaranteeing that the energy production of the concentrated solar thermal plants is not affected by the employment of these new reflectors.

CRediT authorship contribution statement

Francisco Buendía-Martínez: Validation, Investigation, Writing - original draft, Writing - review & editing. **Florian Sutter:** Project administration, Writing - review & editing. **Johannes Wette:** Writing - review & editing. **Loreto Valenzuela:** Project administration, Supervision. **Aránzazu Fernández-García:** Project administration, Funding acquisition, Writing - review & editing, Supervision.

Declaration of competing interest

The authors declare that they have no known competing financial

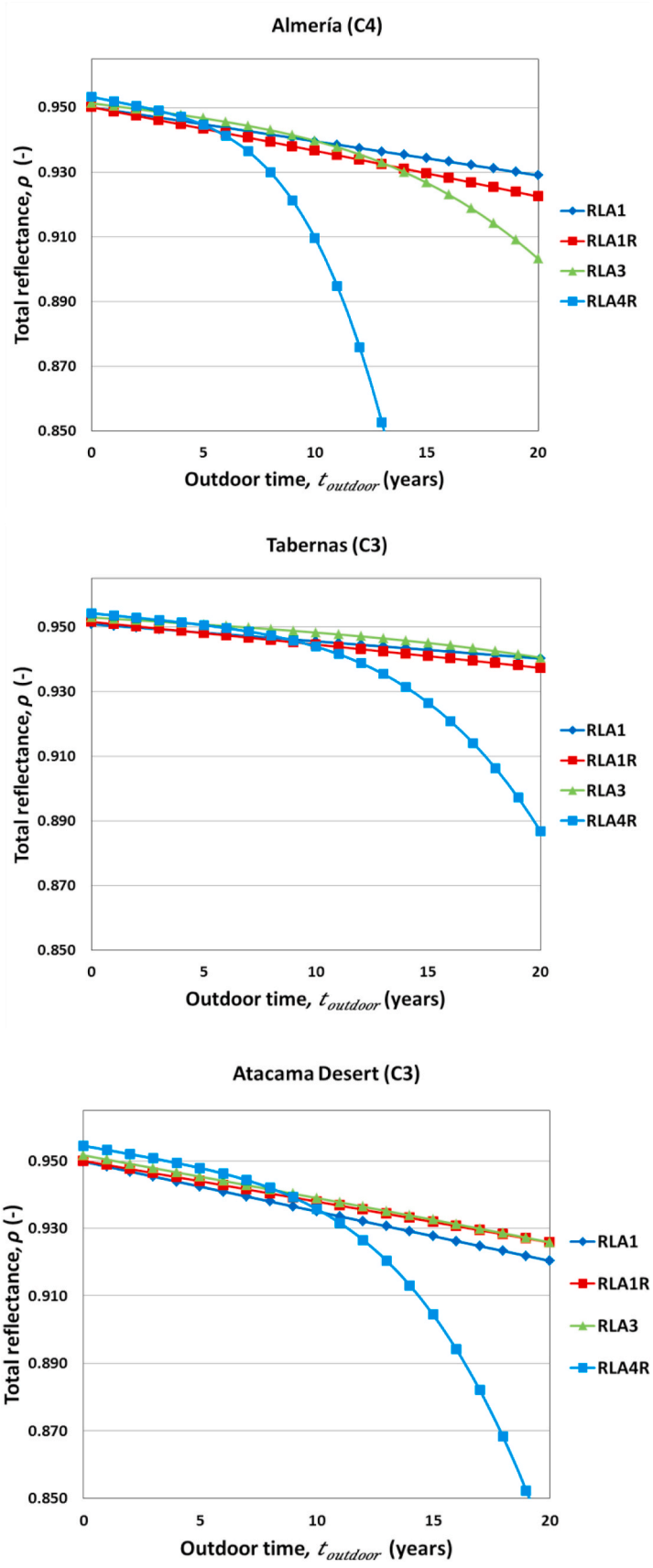

Fig. 10. Prediction of the solar specular reflectance evolution, depending on the material and site.

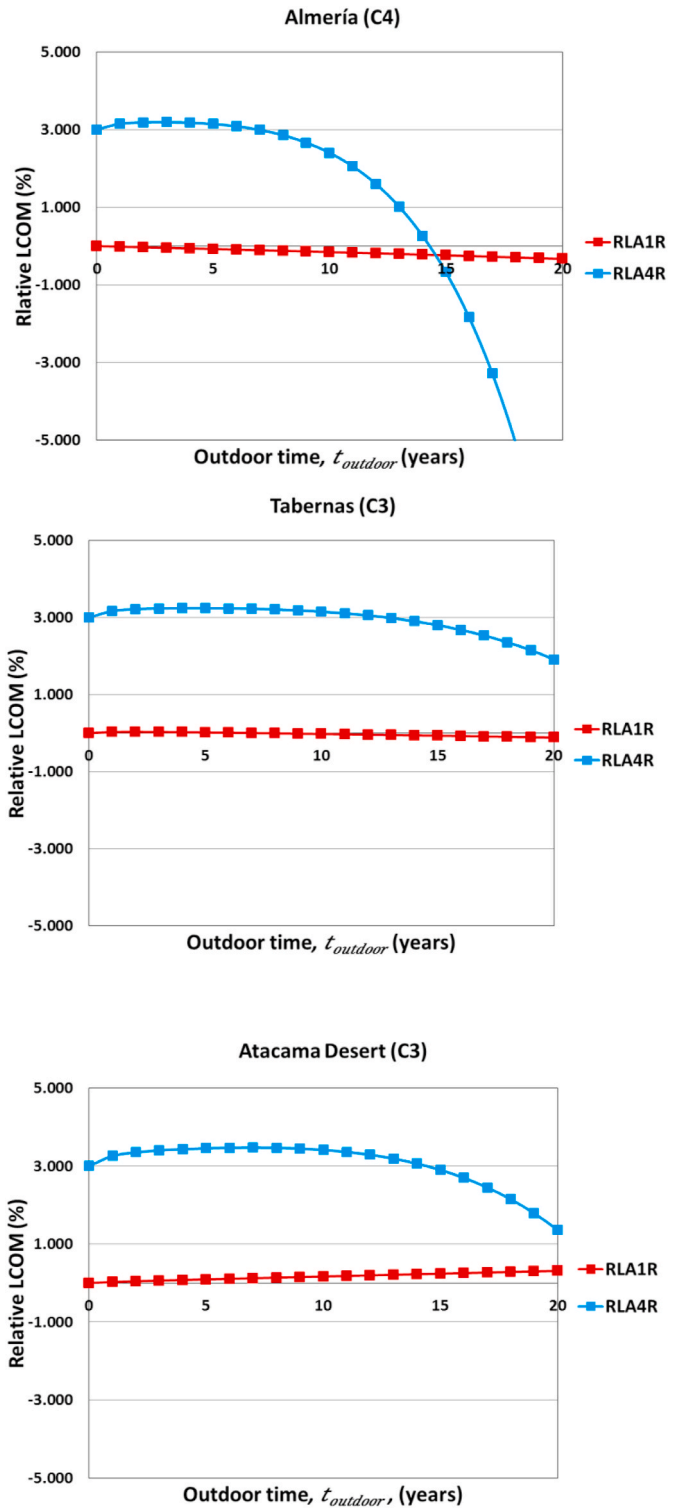

Fig. 11. Relative LCOM in relation to commercial material RLA1, depending on the material and site.

interests or personal relationships that could have appeared to influence the work reported in this paper.

Acknowledgements

This work is part of the project RAISELIFE that has received funding from the European Union's Horizon 2020 research and innovation programme under grant agreement No 686008. Additionally, the research work leading to this article received ERDF funds from the Spanish government within the framework of the SOLTERMIN project (Ref. ENE2017-83973-R) of the Ministerio de Economía, Industria y Competitividad (Spanish Ministry of Economy, Industry and Competitiveness).

The authors would like to thank Iresen and Mascir from Morocco, Plataforma Solar del Desierto de Atacama (PSDA) and Universidad Católica de Chile from Chile, and PROMES-CNRS from France for their valuable contributions in the outdoor exposure process.

References

[1] International Energy Agency, CO2 emissions from fuel combustion: overview, IEA Stat 8 (2017).
[2] Q. Hernández-Escobedo, E. Rodríguez-García, R. Saldaña-Flores, A. Fernández-García, F. Manzano-Agugliaro, Solar energy resource assessment in Mexican states along the Gulf of Mexico, Renew. Sustain. Energy Rev. 43 (2015) 216–238, https://doi.org/10.1016/j.rser.2014.10.025.
[3] A. Jäger-Waldau, Photovoltaics and renewable energies in Europe, Renew. Sustain. Energy Rev. 11 (2007) 1414–1437, https://doi.org/10.1016/j.rser.2005.11.001.
[4] F.G. Montoya, M.J. Aguilera, F. Manzano-Agugliaro, Renewable energy production in Spain: a review, Renew. Sustain. Energy Rev. 33 (2014) 509–531, https://doi.org/10.1016/j.rser.2014.01.091.
[5] T. Tsoutsos, N. Frantzeskaki, V. Gekas, Environmental impacts from the solar energy technologies, Energy Pol. 33 (2005) 289–296, https://doi.org/10.1016/S0301-4215(03)00241-6.
[6] G. Liu, J. Liu, Y. Li, Z. Zhang, J. Chen, et al., Effects of different sizes and dispatch strategies of thermal energy storage on solar energy usage ability of solar thermal power plant, Appl. Therm. Eng. 156 (2019) 14–22, https://doi.org/10.1016/j.applthermaleng.2019.04.041.
[7] Y. Tian, C.Y. Zhao, A review of solar collectors and thermal energy storage in solar thermal, Appl. Energy 104 (2013) 538–553, https://doi.org/10.1016/j.apenergy.2012.11.051.
[8] J. Tomaschek, T. Telsnig, U. Fahl, L. Eltrop, Integrated analysis of dispatchable concentrated solar power, Energy Procedia 69 (2015) 1711–1721, https://doi.org/10.1016/j.egypro.2015.03.138.
[9] International Energy Agency, Renewables Information: Overview 2017, vol. 8, IEA Stat., 2017.
[10] European Solar Thermal Electricity Association (Estela), The Value of Solar Thermal Electricity, 2016.
[11] IRENA, International Renewable Energy Agency, Renewable Power Generation Costs in 2017, 2018, p. 160.
[12] I. Halil, A. Mwesigye, Modeling, simulation and performance analysis of parabolic trough solar collectors: a comprehensive review, Appl. Energy 225 (2018) 135–174, https://doi.org/10.1016/j.apenergy.2018.05.014.
[13] IRENA. International, Renewable Energy Agency, Renewable Energy Technologies: Cost Analysis Series. Concentrating Solar Power, 2012, pp. 1–17.
[14] A. Peinado, A. Pliego, F.P. García Márquez, A review of the application performances of concentrated solar power systems, Appl. Energy 255 (2019) 113893, https://doi.org/10.1016/j.apenergy.2019.113893.
[15] World Bank, Renewable Energy Desalination: an Emerging Solution to Close the Water Gap in the Middle East and North Africa (English), Water Partnership Program (WPP), Washington, DC, 2012.
[16] P. Palenzuela, D.C. Alarcón-Padilla, G. Zaragoza, Large-scale solar desalination by combination with CSP: techno-economic analysis of different options for the Mediterranean Sea and the Arabian Gulf, Desalination 366 (2015) 130–138, https://doi.org/10.1016/j.desal.2014.12.037.
[17] R.S. Schemenauer, H. Fuenzalida, P. Cereceda, A neglected water resource: the Camanchaca of South America, Bull. Am. Meteorol. Soc. 69 (1988) 2.
[18] A. García-Segura, A. Fernández-García, F. Buendía-Martínez, M.J. Ariza, F. Sutter, L. Valenzuela, Durability studies of solar reflectors used in concentrating solar thermal technologies under corrosive sulfurous atmospheres, Sustain. Times 10 (2018) 1–13, https://doi.org/10.3390/su10093008.
[19] A. Fernández-García, R. Díaz-Franco, L. Martinez-Arcos, J. Wette, Study of the effect of acid atmospheres in solar reflectors durability under accelerated aging conditions, Energy Procedia 49 (2014) 1682–1691, https://doi.org/10.1016/j.egypro.2014.03.177.
[20] A. García-Segura, A. Fernández-García, M.J. Ariza, F. Sutter, T. Diamantino, L. Martínez-Arcos, T. Reche-Navarro, L. Valenzuela, Influence of gaseous pollutants and their synergistic effects on the aging of reflector materials for concentrating solar thermal technologies, Sol. Energy Mater. Sol. Cells 200 (2019) 109955, https://doi.org/10.1016/j.solmat.2019.109955.
[21] A. García-Segura, A. Fernández-García, M.J. Ariza, F. Sutter, L. Valenzuela, Effects of reduced sulphur atmospheres on reflector materials for concentrating solar thermal applications, Corrosion Sci. 133 (2018) 78–93, https://doi.org/10.1016/j.corsci.2018.01.021.
[22] A.M. Oje, A.A. Ogwu, S.U. Rahman, A.I. Oje, N. Tsendzughul, Effect of temperature variation on the corrosion behaviour and semiconducting properties of the passive film formed on chromium oxide coatings exposed to saline solution, Corrosion Sci. 154 (2019) 28–35, https://doi.org/10.1016/j.corsci.2019.04.004.

[23] A. Drach, I. Tsukrov, J. DeCew, J. Aufrecht, A. Grohbauer, U. Hofmann, Field studies of corrosion behaviour of copper alloys in natural seawater, Corrosion Sci. 76 (2013) 453–464, https://doi.org/10.1016/j.corsci.2013.07.019.
[24] M. Watanabe, A. Hokazono, T. Handa, T. Ichino, N. Kuwaki, Corrosion of copper and silver plates by volcanic gases, Corrosion Sci. 48 (2006) 3759–3766, https://doi.org/10.1016/j.corsci.2005.12.009.
[25] R. Wiesinger, I. Martina, C. Kleber, M. Schreiner, Influence of relative humidity and ozone on atmospheric silver corrosion, Corrosion Sci. 77 (2013) 69–76, https://doi.org/10.1016/j.corsci.2013.07.028.
[26] F. Sutter, A. Fernández-García, J. Wette, F. Wiesinger, Assessment of Durability and Accelerated Aging Methodology of Solar Reflectors, Modelling, Measurement and Assessment, 2017, pp. 169–201, https://doi.org/10.1016/B978-0-08-100447-0.00006-7.
[27] F. Sutter, J. Wette, F. Wiesinger, A. Fernández-García, S. Ziegler, R. Dasbach, Lifetime prediction of aluminum solar mirrors by correlating accelerated aging and outdoor exposure experiments, Sol. Energy 174 (2018) 149–163, https://doi.org/10.1016/j.solener.2018.09.006.
[28] UNE 206016, Paneles reflectantes para tecnologías de concentración solar, 2018.
[29] ISO 9227, Corrosion tests in artificial atmospheres - salt spray tests, 2017.
[30] Y. Peiyun, L. Xiaobo, Y. Li, F. Fan, P. Linfa, L. Xinmin, A lifetime prediction model for coated metallic bipolar plates in proton exchange membrane fuel cells, Energy, Convers. Manag. 183 (2019) 65–72, https://doi.org/10.1016/j.enconman.2018.12.092.
[31] Y.J. Cui, B.L. Wang, J.E. Li, K.F. Wang, Performance evaluation and lifetime prediction of a segmented photovoltaic-thermoelectric hybrid system, Energy Convers. Manag. 211 (2020) 112744, https://doi.org/10.1016/j.enconman.2020.112744.
[32] H. Zunyan, X. Liangfei, L. Jianqiu, O. Minggao, S. Ziyou, H. Haiyan, A reconstructed fuel cell life-prediction model for a fuel cell hybrid city bus, Energy Convers. Manag. 156 (2018) 723–732, https://doi.org/10.1016/j.enconman.2017.11.069.
[33] F. Sutter, S. Ziegler, M. Schmücker, P. Heller, R. Pitz-Paal, Modelling of optical durability of enhanced aluminum solar reflectors, Sol. Energy Mater. Sol. Cells 107 (2012) 37–45, https://doi.org/10.1016/j.solmat.2012.07.027.
[34] M.J. Digrazia, W. Highway, R. Gee, W. Highway, G. Jorgensen, W. Highway, et al., Wref 2012: Service Life Prediction for Reflectech Mirror Film, 2012.
[35] ISO 9223, Corrosion of Metals and Alloys - Corrosivity of Atmospheres - Classification, Determination and Estimation, 2012.
[36] A. García-Segura, A. Fernández-García, M.J. Ariza, F. Sutter, L. Valenzuela, Durability studies of solar reflectors: a review, Renew. Sustain. Energy Rev. 62 (2016) 453–467, https://doi.org/10.1016/j.rser.2016.04.060.
[37] F. Wiesinger, F. Sutter, F. Wolfertstetter, N. Hanrieder, J. Wette, A. Fernandez-Garcia, R. Pitz-Paal, Sandstorm erosion simulation on solar mirrors and comparison with field data, AIP Conference Proceedings 1850 (2017), https://doi.org/10.1063/1.4984508.
[38] J. Wette, F. Sutter, A. Fernández-García, S. Ziegler, R. Dasbach, Comparison of degradation on aluminum reflectors for solar collectors due to outdoor exposure and accelerated aging, Energies 9 (2016) 916, https://doi.org/10.3390/en9110916.
[39] J. Wette, F. Sutter, M. Tu, A. Fernández-García, F. Buendia-Martinez, M. J. Carvalho, T. Diamantino, Advanced cyclic accelerated aging testing of solar reflector materials, AIP Conference Proceedings 2126 (2019), https://doi.org/10.1063/1.5117670.
[40] P. Heller, The performance of concentrated solar power (CSP) systems: analysis, Chap 3: Mirrors, Measurement and Assessment (2017) 67–98.
[41] F. Buendía-Martínez, A. Fernández-García, F. Sutter, L. Valenzuela, A. García-Segura, Advanced analysis of corroded solar reflectors, Coatings 9 (2019) 749, https://doi.org/10.3390/coatings9110749.
[42] F. Sutter, A. Fernández-García, M. Montechhi, Indirect method to determine near-normal sun-conic reflectance, Solarpaces conference (2019).
[43] A. Fernández-García, F. Sutter, L. Martínez-Arcos, C. Sansom, F. Wolfertstetter, C. Delord, Equipment and methods for measuring reflectance of concentrating solar reflector materials, Sol. Energy Mater. Sol. Cells 167 (2017) 28–52, https://doi.org/10.1016/j.solmat.2017.03.036.
[44] F. Buendía-Martínez, A. Fernández-García, F. Sutter, L. Martínez-Arcos, T. Reche-Navarro, A. Garcia-Segura, L. Valenzuela, Uncertainty study of reflectance measurements for concentrating solar reflectors, IEEE Trans. Instrum. Meas. (2020), https://doi.org/10.1109/TIM.2020.2975387.
[45] ISO 9050, Glass in Building — Determination of Light Transmittance, Solar Direct Transmittance, Total Solar Energy Transmittance, Ultraviolet Transmittance and Related Glazing Factors, 2003.
[46] ASTM G173-03, Standard Tables for Reference Solar Spectral Irradiances: Direct Normal and Hemispherical on 37° Tilted Surface, 2012.
[47] F. Wiesinger, F. Sutter, A. Fernandez-Garcia, J. Wette, F. Wolfertstetter, N. Hanrieder, M. Schmücker, R. Pitz-Paal, Sandstorm erosion on solar reflectors: highly realistic modeling of artificial aging tests based on advanced site assessment, Appl. Energy 268 (2020) 114925, https://doi.org/10.1016/j.apenergy.2020.114925.
[48] M. Karim, S. Naamane, I. El Amrani El Hassani, C. Delord, S. Belcadi, P. Tochon, A. Bennouna, Towards the prediction of CSP mirrors wear: methodology of analysis of influencing parameters on the mirrors surface degradation: application in two different sites in Morocco, Sol. Energy 108 (2014) 41–50, https://doi.org/10.1016/j.solener.2014.06.036.
[49] X. Zhuang, X. Xinhai, L. Wenrui, X. Wenfu, LCOE analysis of tower concentrating solar power plants using different molten-salts for thermal energy storage in China, Energies 12 (2019) 1394, https://doi.org/10.3390/en12071394.
[50] S. Boukheir et al. reportRaiselife Deliverable D1.3: Report on Outdoor Exposure of Mirror Samples.
[51] F. Sutter, A. Fernández-García, P. Heller, K. Anderson, G. Wilson, M. Schmücker, P. Marvig, Durability testing of silvered-glass mirrors, Energy Procedia 69 (2015) 1568–1577, https://doi.org/10.1016/j.egypro.2015.03.110.
[52] M. Köhl, B. Carlsson, G.J. Jorgensen, A.W. Czanderna, Performance and Durability Assessment Optical Material for Solar Thermal Systems, 1st., Elsiever, 2004.